Quasi-Optical Optimization and Modal Analysis of Cornercube Schottky-Diode Mixers

J. Brune, P. Bierschneider

Laboratories for High Frequency Technology
University Erlangen-Nürnberg
Cauerstr.9
D-90518 Erlangen. Federal Republic of Germany

Abstract

An optimization of the system cornercube mixer - Gaussian beam requires a calculation of the power coupling coefficient. First, the cornercube field is determined by the use of image theory. Then the field of a Gaussian beam is transformed into the cornercube coordinate system. The transformation used here allows both: a tilt of the mixer relative to the beam and also longitudinal and lateral shifts. Now the evaluation of the coupling integral will be performed numerically.

The optimization of the beam parameters for the standard cornercube mixer ($L = 4\lambda$, $s = 1.2\lambda$) and for a commercially available mixer ($L = 4\lambda$, $s = 0.93\lambda$) resulted in maximum power coupling coefficients of 59 % and 77 % respectively. If the antenna dimensions are also involved in the optimization process a coupling of 88 % can be reached for an antenna configuration with $L = 0.92\lambda$ and $s = 0.83\lambda$. Finally the frequency response is shown and a modal analysis is performed for all three mixer types. It can be concluded that the standard configuration used in many quasi-optical systems all over the world is far away from the optimum.

1 Introduction

Schottky-diode mixers of the cornercube-type are still widely used in quasi-optical submillimeterwave systems for radioastronomy [1], plasma diagnostics [2] and environmental monitoring [3]. While waveguide Schottky mixers [5] and SIS mixers are limited to about 700 GHz, Cornercube mixers are currently employed in radiometer systems for frequencies up to 2.5 THz and higher [4]. However, waveguide mixers provide a better coupling to Gaussian beams if equipped with suitable horn antennas. The intention of this paper is to provide an insight in the coupling calculations and the parameters which influence the coupling of a cornercube and a Gaussian beam. Suggestions will be given how the performance of existing cornercube mixers can easily be improved.

After the invention of the whisker antenna in 1970 by MATARRESE et.al. [6], in 1977 KRÄUTLE et.al. [7],[8] started to improve the coupling between the field

of a Gaussian beam and the whisker antenna field by placing rooftop-reflectors behind the antenna. The spacing between the antenna and the rooftop reflector and the opening angle of the rooftop was experimentally optimized in order to get a round main lobe which was believed to give the best coupling to a Gaussian beam. The optimisation resulted in a 4λ whisker antenna spaced 1.2λ from a 90°-rooftop reflector. This design is still used as a "cookbook recipe" all around the world and will be referred to as the "standard configuration" in this paper. In 1984 HERRMANN [9] calculated the coupling between a Gaussian beam and a Schottky diode mixer in rooftop configuration for the first time. He found that the coupling is about 50 %. However, the calculations only involved the amplitudes of the two fields. In the analysis of KELLY et.al. [10] in 1985 the rooftop mixer was analyzed and practical suggestions for the mixer design and fixture were given. GROSSMAN [11] performed in 1989 an evaluation of the coupling integral for a 90°-rooftop reflector. He could show that the standard configuration is in no sense optimal and gave recommendations for improved antenna dimensions in a 90°-rooftop reflector.

However, most of the open structure Schottky diode mixers are rather in a cornercube than in a rooftop configuration, this means that an additional ground reflector is employed which influence has been neglected in the former studies. Additionally the radiation attenuation and shifts of the input coupling Gaussian beam along the cartesian coordinate axes were not taken into account up to now. These factors will be included in our cornercube model we present in the following.

2 Field calculations

Fig. 1 shows the geometry of a typical cornercube configuration. The whisker antenna with length L stands vertically on the ground reflector and is spaced at a distance s from the apex of the 90° rooftop reflector. On the bottom of the antenna the diode chip is placed on a choke structure (for design optimization of the choke structure see [12]). A Gaussian beam is focused onto the cornercube, the variable beam parameters are the waist position in space, the waist radius and the direction of propagation.

The calculation of the coupling between the incoming Gaussian beam and the antenna structure will be performed in different steps: First, the electric fields of the cornercube and the Gaussian beam are required. The antenna field will be determined according to the reciprocity principle [13] for the case of a load-independent current wave with amplitude I_0. The electrical field of the Gaussian beam will then be transformed into the same spherical polar coordinate system as the cornercube. Now, the coupling integral [14] can be evaluated numerically.

2.1 Cornercube mixer

Before the corner reflector is taken into account, the electrical field $\vec{E}_W$ of a free standing single longwire whisker-antenna of length L is required. It can be shown

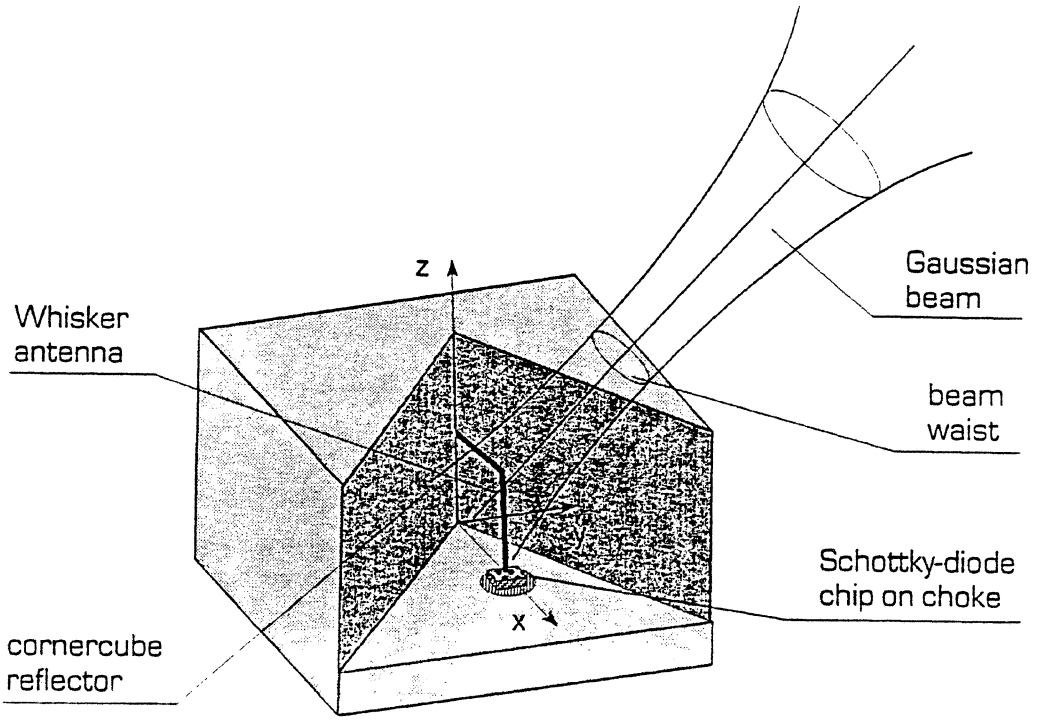

Figure 1: Quasi-optical cornercube Schottky-diode mixer

that only the z-component exists [9]:

$$E_{z\,W}(r,\vartheta,\varphi) = -\frac{\mu_0 I_0 L}{4\pi r}\cdot\exp\{-jkr\}\cdot j\omega\cdot \cdot\frac{\exp\{jkL(\cos(\vartheta)-1)-\alpha L\}-1}{jkL(\cos(\vartheta)-1)-\alpha L}\cdot\exp\{j\omega t\} \quad (1)$$

Eq.(1) is given in a mixed representation of cylindrical and spherical polar coordinates. The dependence on spherical polar coordinates is useful because the evaluation of the coupling integral will be performed over a spherical surface, while the scalar product between the fields of the cornercube and the Gaussian beam is easier to perform with the z-component instead of a superposition of the r- and ϑ-components. The ϑ-component of the whisker field alone is not sufficient for the coupling calculations because translational shifts of the Gaussian beam will also be allowed during mixer optimization. From Eq.(1) one sees that the electric field is independent of φ, it is therefore axially symmetric to the z-axis. In Fig. 2 the antenna pattern of a 4λ longwire whisker-antenna is displayed.

This axially symmetric beam pattern can be shaped by introducing plane reflectors around the antenna in order to give a main lobe and therefore to improve the coupling to a Gausian beam. While in the beginning of the development of the standard configuration only one rooftop-mirror was employed, nowadays most of the open-structure mixers have an additional ground reflector for mechanical and optical reasons. The influence of this ground reflector must not be neglected.

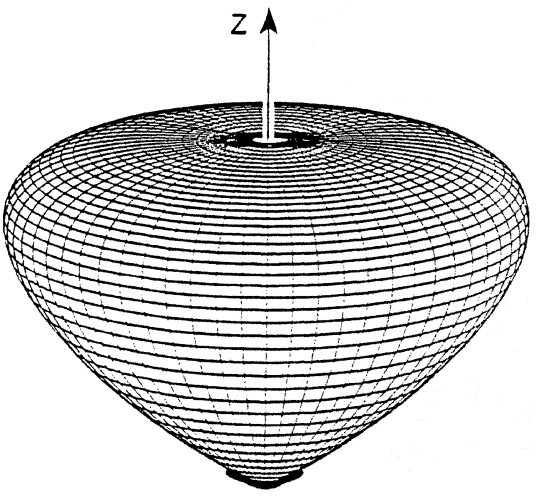

Figure 2: Linear antenna pattern of a 4λ whisker-longwire-antenna

With the theory of images the influence of the reflectors can be determined: the whisker antenna and its images will be considered as an antenna group [15] and the electric field can be calculated by a proper superposition of the single antenna fields. However, the current wave will have a different sign depending on whether the antenna is parallel or perpendicular to the reflector plane. In Fig. 3 the relevant cases for a reflection of the whisker antenna on a plane reflector are displayed: corresponding to the static case the current wave on the image antennas will be of opposite sign. The case of the whisker being parallel to the reflector plane can therefore be replaced by a real whisker antenna with positive sign of its current wave and the image antenna with negative sign. Both waves are travelling in the same direction (Fig. 3a)). If the whisker is standing perpendicular on the reflector as in the case of the ground reflector, the image current wave is of opposite sign and travels into opposite direction (Fig. 3b)). In the case of a rooftop reflector also a second reflection of the two negative image antennas occurs which finally results in a positive current wave on the resulting image antenna (Fig. 3c)).

Fig. 4 shows the case of the cornercube mixer configuration. The influence of the whisker and its seven images have to be superimposed with proper sign and phase. Advantage can be taken out of Fig. 3 b): with Eq. (1) the influence of the four image antennas below the ground reflector can be taken into account as follows, where $E_{z\,CC}$ represents the field of the cornercube and $E_{z\,RT}$ the field of the rooftop configuration, i.e. the four antennas above the ground reflector:

$$E_{z\,CC}(r,\vartheta,\varphi) = E_{z\,RT}(r,\vartheta,\varphi) + E_{z\,RT}(r,(\pi-\vartheta),\varphi) \qquad (2)$$

To determine the field $E_{z\,RT}$ the fields of the real whisker antenna and its three images will be superimposed. By using the far field approximation only the different phases of the antennas in a distant point P will be considered. This can be done by multiplying the field $E_{z\,W}$ of the whisker antenna with the additional phase shifts

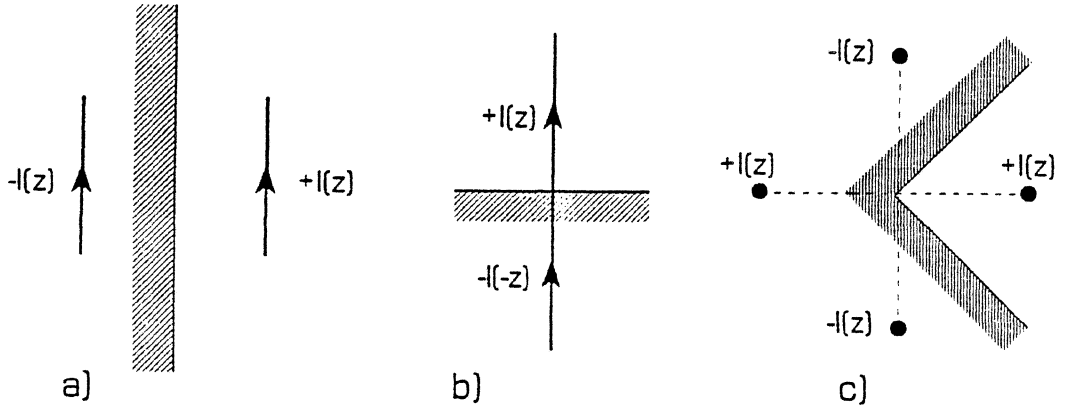

Figure 3: Reflection of the whisker-antenna at plane reflectors
a) whisker antenna parallel to the reflector plane
b) whisker antenna perpendicular to the reflector plane
c) Rooftop-reflector (from above)

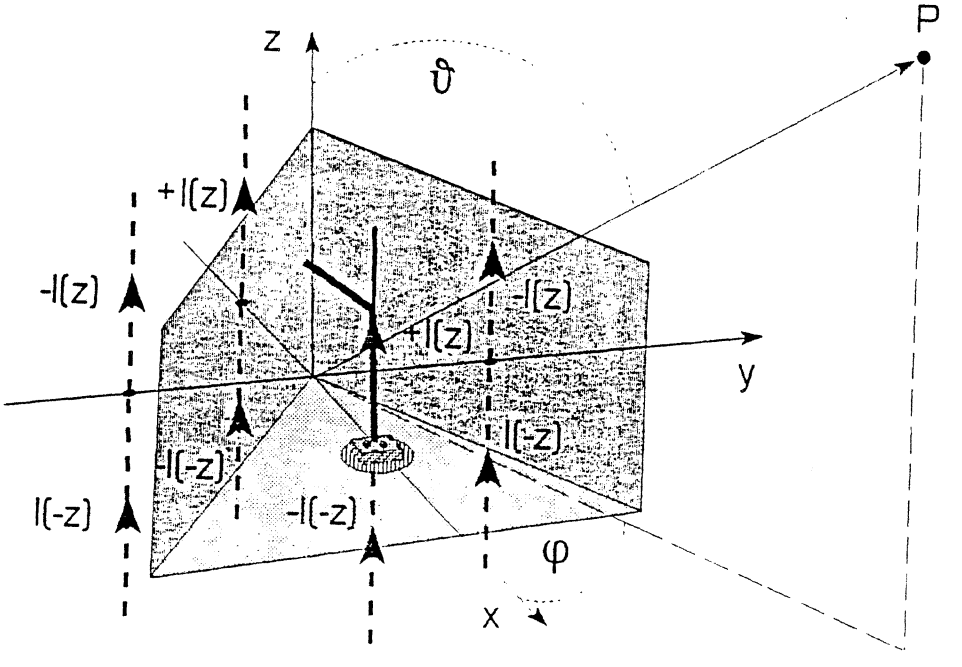

Figure 4: Whisker antenna and its images in a cornercube mixer configuration

Φ^n of each single antenna in the distant point P. The amplitude differences in P will be neglected because the distance from the antennas to P is much larger than the distances of the antennas from each other.

$$E_{z\,RT}(r,\vartheta,\varphi) = \sum_{n=1}^{4} E_z^n{}_W(r,\vartheta,\varphi) \approx E_{z\,W}(r,\vartheta,\varphi) \sum_{n=1}^{4} \Phi^n \tag{3}$$

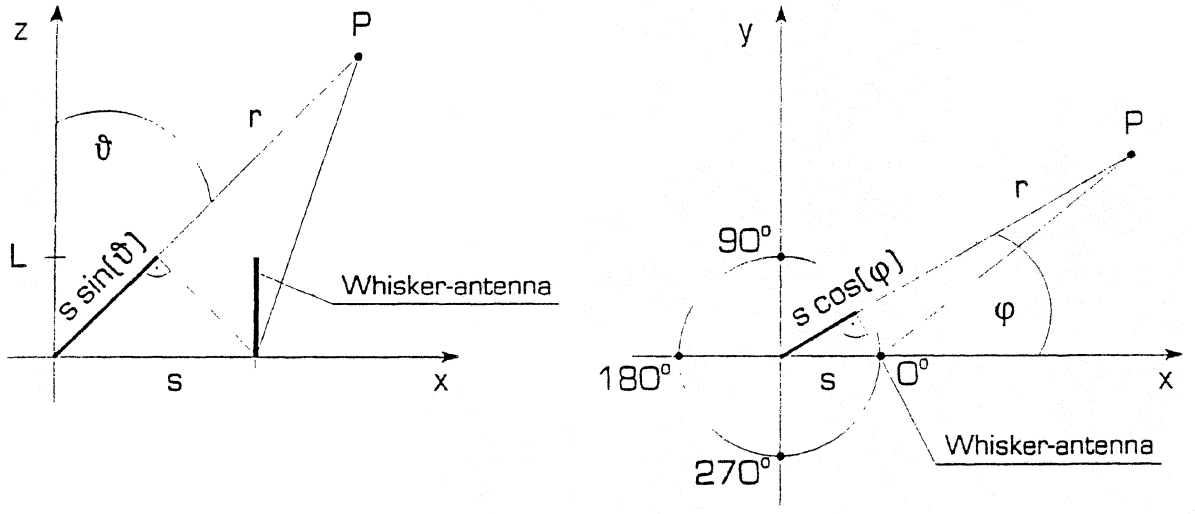

Figure 5: Phase differences of the four single antennas in a distant point P with respect to the origin

Fig. 5 explains, where the phase differences of the four antenna fields in a distant point P come from. The origin of the coordinate system from Fig. 4 will be used as reference point. Under consideration of the current signs corresponding to Fig. 3 one obtains for the four phases:

$$\Phi^1 = +\exp\{+jks\sin(\vartheta)\cos(\varphi)\} \tag{4}$$
$$\Phi^2 = -\exp\{+jks\sin(\vartheta)\cos(\varphi - 90^0)\} \tag{5}$$
$$\Phi^3 = +\exp\{+jks\sin(\vartheta)\cos(\varphi - 180^0)\} \tag{6}$$
$$\Phi^4 = -\exp\{+jks\sin(\vartheta)\cos(\varphi - 270^0)\} \tag{7}$$

With these four additional phase shifts the electrical field $E_{z\,RT}(r,\vartheta,\varphi)$ of the rooftop-configuration, i.e. the four upper antennas will now be determined according to Eq. 3.

$$\begin{aligned} E_{z\,RT}(r,\vartheta,\varphi) &= \\ &= E_{z\,W}(r,\vartheta,\varphi) \cdot \sum_{n=1}^{4} \Phi^n \qquad (8) \\ &= 2E_{z\,W}(r,\vartheta,\varphi)\{\cos(ks\sin(\vartheta)\cos(\varphi)) - \cos(ks\sin(\vartheta)\sin(\varphi))\} \end{aligned}$$

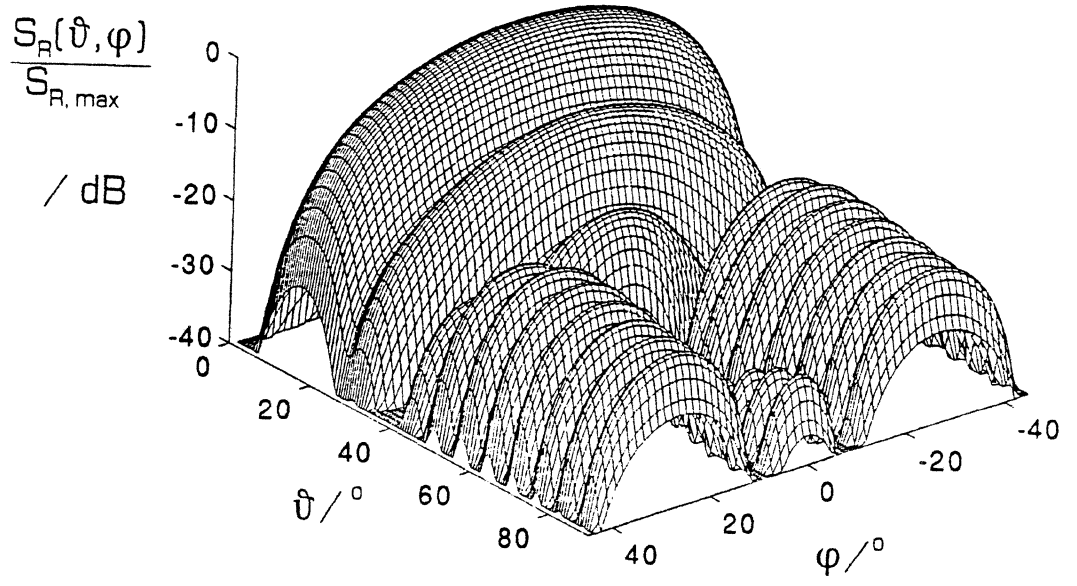

Figure 6: Calculated antenna pattern for a cornercube mixer in standard configuration ($L = 4\lambda$; $s = 1,2\lambda$)

With Eq.(2) and $\omega = kc$ one finally gets the electric field of the rooftop mixer configuration.

$$
\begin{aligned}
& E_{z\,CC}(r,\vartheta,\varphi) = \\
& = \frac{\mu_0 I_0 c}{2\pi r} \cdot j \cdot \exp\{-jkr\} \cdot \exp\{j\omega t\} \\
& \cdot \{\cos(ks\sin(\vartheta)\cos(\varphi)) - \cos(ks\sin(\vartheta)\sin(\varphi))\} \\
& \cdot \left[\frac{\exp\{-jkL(\cos(\vartheta)+1) - \alpha L\} - 1}{j(\cos(\vartheta)+1) + \alpha/k} - \frac{\exp\{jkL(\cos(\vartheta)-1) - \alpha L\} - 1}{j(\cos(\vartheta)-1) - \alpha/k}\right]
\end{aligned}
\tag{9}
$$

In Fig. 6 the calculated antenna pattern of a cornercube mixer in standard configuration ($L = 4\lambda$; $s = 1,2\lambda$) is shown. Note that a distorted representation of the two angles ϑ and φ is given instead of a depiction in polar coordinates.

2.2 Gaussian beam

The electrical field for a linearily polarized fundamental Gaussian beam mode will be extracted from the literature (e.g. [16]). For the transversal field component of a fundamental mode which travels along the $+z'$-axis and which is polarized in x'-direction one gets:

$$
E_{00_{x'}} = u_{00} \cdot e^{-jkz'} \cdot e^{j\omega t} \tag{10}
$$

with

$$u_{00}(x',y',z') = \sqrt{\frac{2}{\pi}}\frac{1}{w}\cdot\exp\left[\frac{-(x'^2+y'^2)}{w^2}\right]\cdot\exp\left[-j\frac{k(x'^2+y'^2)}{2R}\right]\cdot\exp\left[i(\varphi+\varphi_0)\right] \tag{11}$$

and

$$w^2 = w_0^2\cdot\left[1+\left(\frac{2(z'-z_0')}{kw_0^2}\right)^2\right] \tag{12}$$

$$R = \frac{k^2w_0^4}{4(z'-z_0')}+(z'-z_0') \tag{13}$$

$$\varphi = \arctan\left\{\frac{2(z'-z_0')}{kw_0^2}\right\} \tag{14}$$

For the modal analysis performed later, also higher order beam modes are required. In this paper Hermite-Gaussian (HG) beam modes will be used, although the generalized Laguerre-Gaussian (LG) modes are fully equivalent (the transformation relations between HG and LG modes can be found in [17]). With Eq.(11) one gets for the HG-Modes:

$$u_{mn}(x',y',z') = \left\{\frac{1}{2^{n+m}n!m!}\right\}^{\frac{1}{2}}\cdot H_m\left[\sqrt{2}\frac{x'}{w}\right]\cdot H_n\left[\sqrt{2}\frac{y'}{w}\right]\cdot \cdot\exp\left\{j(m+n)\varphi\right\}\cdot u_{00}(x',y',z') \tag{15}$$

2.3 Coordinate transformation

In Fig. 7 the location of the coordinate system (x,y,z) of the cornercube mixer relative to the coordinate system (x',y',z') of the Gausian beam is shown. For the determination of the coupling integral the (x',y',z') system has to be transformed into the system (x,y,z) of the cornercube mixer. The origins of the (x,y,z)- and the (x',y',z')-systems are coincident, however they are tilted by the angles ϑ_G and φ_G which represent the incoming angle of the Gaussian beam. Finally, the position of the beam waist is determined by the point $P_0(x_0',y_0',z_0')$. With these definitions the transformation relations can be given:

$$\begin{aligned} x' &= -x\cos(\vartheta_G)\cos(\varphi_G) - y\cos(\vartheta_G)\sin(\varphi_G) + z\sin(\vartheta_G) - x_0' \\ y' &= -x\sin(\varphi_G) + y\cos(\varphi_G) - y_0' \\ z' &= -x\sin(\vartheta_G)\cos(\varphi_G) - y\sin(\vartheta_G)\sin(\varphi_G) - z\cos(\varphi_G) - z_0' \end{aligned} \tag{16}$$

2.4 Evaluation of the coupling integral

The coupling integral Eq.(17) gives the amount of power coupled from one antenna field (transmitter) into the other (receiver) [14]. In our case the electrical field $\vec{E}_{mn}$

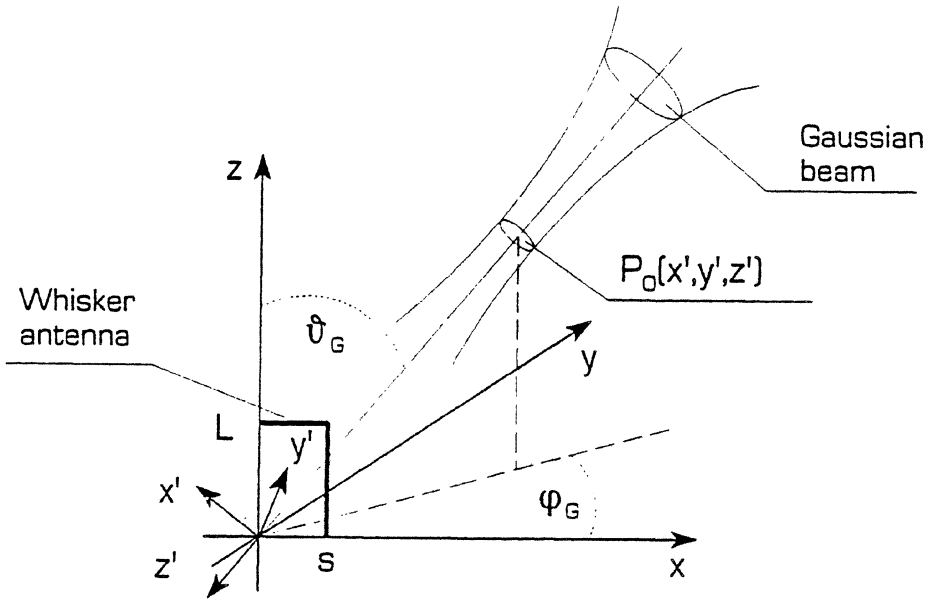

Figure 7: Location of the coordinate system (x, y, z) of the cornercube antenna relative to the coordinate system (x', y', z') of the Gausian beam

of the Gaussian beam mode of order m, n can be considered as the transmitter field while the cornercube antenna field $\vec{E_{CC}}$ is the receiver field:

$$K_{mn} = \frac{\left| \int\int_A \vec{E_{CC}} \cdot \vec{E}_{mn}^{*} \, dA \right|^2}{\left[\int\int_A | \vec{E_{CC}} |^2 \, dA \right] \left[\int\int_A | \vec{E}_{mn} |^2 \, dA \right]} \tag{17}$$

The integration will be evaluated over an octant $-\pi/4 < \phi < \pi/4$ and $0 < \vartheta < \pi/2$ of a sphere with radius r_i because the cornercube field disappears outside this area. By numerical investigations it was found that the integration radius r_i should be chosen between 32λ and 128λ. If the value of r_i is too big the paraxial approximation is no longer valid. Too small values of r_i cause the far field approximation to be hurt. For the coupling calculations we finally chose $r_i = 100\lambda$ and 2500 integration points.

3 Optimization of the beam coupling to Cornercube mixers

During the quasi-optical optimization of the cornercube mixer the beam parameters and the antenna dimensions will be affected. The beam parameters are the waist radius w_0, the beam waist position in space and the direction of beam propaga-

tion. The latter are described by the angles ϑ_G, φ_G and the beam waist position $P_0(x', y', z')$ as given in Fig. 7. This representation was chosen because it represents the situation in practical mixer adjustment: in most cases the mixer itself instead of the incoming Gaussian beam will be adjusted. First the mixer mount will be tilted by the angles ϑ_G and φ_G relative to the Gaussian beam in order to increase video response or to decrease the noise temperature respectively. Then, the tilted mixer will be translationally shifted in order to maximize the mixer performance, i.e. a fine adjustment along the cartesian coordinate axes (x', y', z') of the coordinate system of the Gaussian beam will be performed.

From the range of possible mixer parameters only the antenna length L and the spacing s between the antenna and the apex of the corner reflector will be involved in the optimization process because only the whisker has to be changed for improving the mixer while the mixer housing can be reused. Therefore the opening angle of the apex will be kept constant at an angle of 90°. According to experimentally obtained values [9] the radiation attenuation will be set to 200 m^{-1}. With Eq. (11) the power coupling factor K_{00} of the cornercube field and the fundamental Gaussian beam mode can now be calculated.

The optimizations were performed on a standard PC in TURBO PASCAL. In our program all the mixer and beam parameters can be changed. However due to long computing times not more than two parameters have been varied at once in practical operation After an optimum has been found, two other parameters have been chosen. This procedure will be performed until the optimum is reached. A problem is the presence of local maxima: an optimization towards those relative maxima can be avoided by performing several optimizations with different starting values and by repeating the optimization procedure several times.

First the radiation resistance R_S was determined for different antenna dimensions L and s. Its value is important for the coupling between the antenna and the Schottky diode and strongly influences the performance of the mixer. With the Poynting vector $\vec{S}_r$ the integration surface A around the antenna, the free-space wave resistance Z_0 and the impressed current I_0, R_S is defined by

$$R_S = \frac{\iint_A \vec{S}_r \cdot d\vec{A}}{|I_0|} = \frac{\iint_A |E_z|^2 \sin^2(\vartheta)\, dA}{Z_0 |I_0|^2} \tag{18}$$

In Fig. 8 the radiation resistance is depicted depending on L and s. The significant difference in comparison to the diagram of GROSSMAN [11] is caused by the influence of the radiation attenuation and the ground reflector and shows the importance of considering them.

After these calculations the optimum beam parameters for two given mixer configurations were determined: for the standard configuration ($l = 4\lambda$: $s = 1,2\lambda$) and for a commercially available cornercube mixer [18] ($l = 4\lambda$: $s = 0,93\lambda$). Starting with these given antenna parameters the beam parameters were gradually changed in order to maximize K_{00}. In a third case also the antenna dimensions were changed during the optimization process. This procedure finally results in an optimum mixer configuration. The results are given in Tab. 1

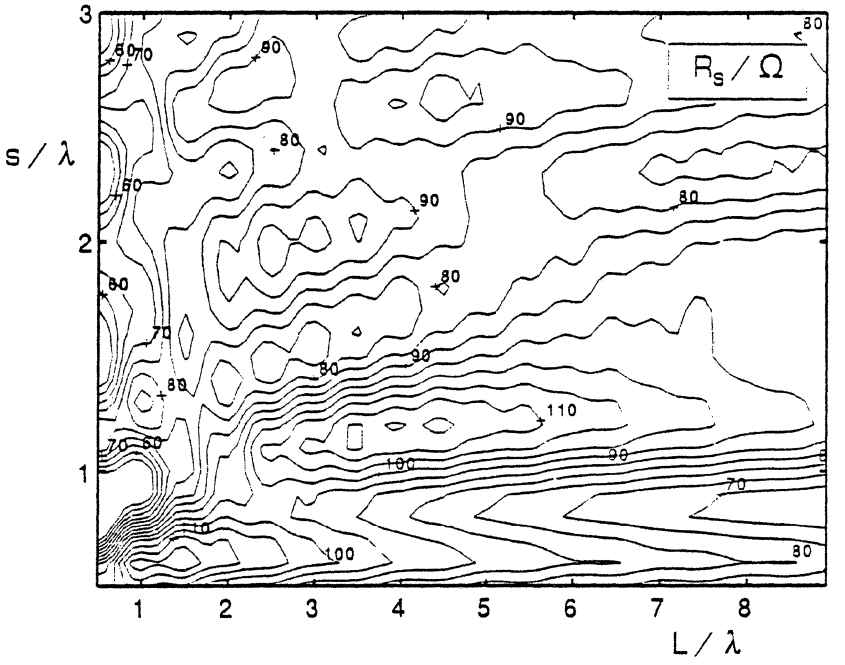

Figure 8: Radiation resistance R_S depending on the relative whisker length l/λ and the relative whisker spacing s/λ

From Tab. 1 we can easily extract that the optical coupling efficiency of the standard mixer configuration can be highly exceeded by the commercial and the optimum configurations. The coupling of the whisker-antenna to the Schottky diodes however, will decrease if a mismatch between the radiation resistance R_S and the diode impedance R_D occurs. To account for this effect, we define the overall coupling efficiency $K_{\text{tot.}}$:

$$K_{\text{tot.}} = K_{\text{DA}} \cdot K_{00} \tag{19}$$

with the coupling efficiency due to diode-antenna mismatch [9] K_{DA}:

$$K_{\text{DA}} = 1 - \left| \frac{R_D - R_S}{R_D + R_S} \right|^2 \tag{20}$$

The diode impedance R_D is dependent on many parameters including LO power and bias current. For most submillimeterwave mixers with Schottky diodes R_D can be estimated to lie between 100Ω and 200Ω [9]. For our calculations the more optimistic value $R_D = 100\Omega$ was used. The resulting coupling efficiencies are given in the last column of Tab. 1. The difference between the optimum and the commercial mixer is only about 5 %. It can however be expected that beam distortion occurs due to $w_0/\lambda < 1$. We therefore recommend the use of the commercial configuration.

The differences between the different mixer configurations can even more clearly be seen if we look at the frequency dependence of the quasi-optical power coupling coefficient. In Fig. 9 the three mixer types are compared for the case of a design for the center frequency $f = 600$ GHz. The beam parameters have been optimized for maximum optical coupling at the design frequency and have been kept constant over

	design parameter	Mixer type		
		standard	commercial	optimum
antenna parameters	L/λ	4.0	4.0	0.92
	s/λ	1.2	0.93	0.83
	$\alpha[\mathrm{m}^{-1}]$	200	200	200
beam parameters	w_0/λ	1.66	1.46	1.01
	$\vartheta[^\circ]$	24	26.5	44.5
	$\varphi[^\circ]$	0	0	0
	x_0'/λ	−0.7	−0.6	−0.25
	y_0'/λ	0	0	0
	z_0'/λ	2	1.6	4.12
optimization results	R_S/Ω	115	91	59
	Quasi-optical Coupling Efficiency K_{00}	59.5 %	77.2 %	88.0 %
	Overall Coupling Efficiency $K_{\mathrm{tot.}}$	59.2 %	77.0 %	82.1 %

Table 1: Optimization of the quasi-optical coupling to cornercube mixers

the varied frequency. This is typical for frequency independent quasioptical setups where no adjustments during operation will be performed (e.g. [19]). It can clearly be seen that the standard configuration is not at all an optimum one: it reaches its maximum coupling at lower frequencies, where the relative antenna length L/λ is shorter. The performance of the commercially available mixer is again closer to the optimum.

From Tab. 1 it can also be seen that it is worth not only to allow rotational but also translational adjustment in mixer fixtures. The 3-dB adjustment tolerances lie within some tenths of the wavelength and a few degrees respectively for all given parameters. Therefore care should be taken when designing the mixer fixture.

At last a modal analysis of the three mixer types was performed by evaluating the coupling integral Eq. 17 for the higher order modes instead of the fundamental mode. The beam parameters have been extracted from Tab. 1. In the following modal tables Tab. 2 to Tab. 4 power distribution on the first 100 Gauß-Hermite modes is given. In the caption the amount of power P_{sum} contained in these first 100 modes is given relative to the total radiated power by the cornercube mixer P_{CC}. One can see that a significant amount of beam power is contained outside the Gaussian (paraxial) regime for the standard mixer while for the optimum mixer the field can be better represented by Gaussian beams.

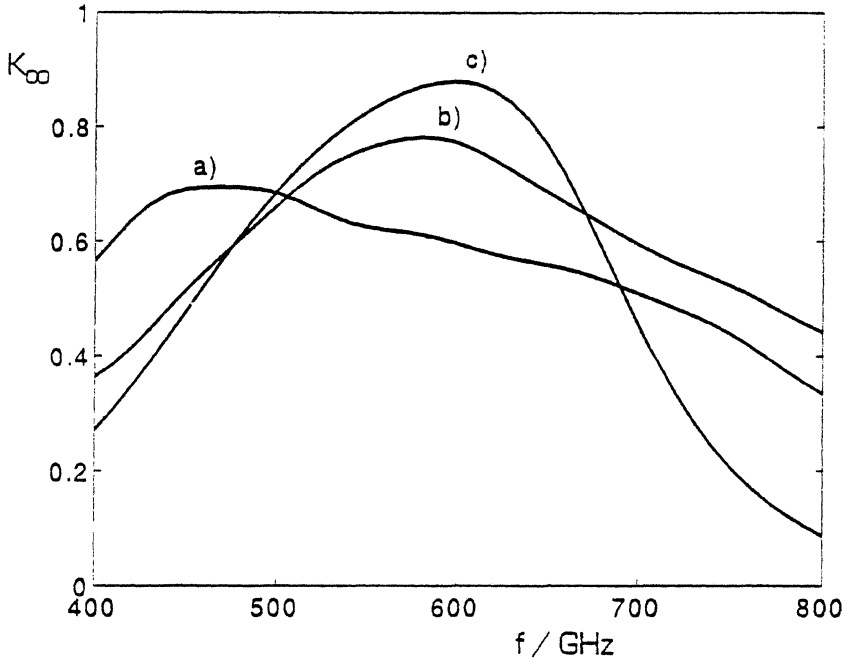

Figure 9: Frequency dependence of the quasi-optical coupling to cornercube mixers for the case of optimum coupling
a) standard configuration ($L = 4\lambda$, $s = 1.2\lambda$)
b) commercial configuration ($L = 4\lambda$, $s = 0.93\lambda$)
c) optimum configuration ($L = 0.92\lambda$, $s = 0.83\lambda$)

m n	0	1	2	3	4	5	6	7	8	9
0	0.5952	0	0.0037	0	0.0014	0	0.0002	0	0.0001	0
1	0.0001	0	0	0	0	0	0.0001	0	0.0001	0
2	0.0030	0	0.0042	0	0.0005	0	0.0004	0	0.0001	0
3	0.0008	0	0.0001	0	0.0007	0	0.0004	0	0.0004	0
4	0.0005	0	0.0001	0	0.0003	0	0.0002	0	0.0003	0
5	0.0001	0	0.0006	0	0.0006	0	0.0008	0	0.0005	0
6	0.0003	0	0.0005	0	0.0005	0	0.0007	0	0.0006	0
7	0.0001	0	0.0006	0	0.0009	0	0.0007	0	0.0006	0
8	0	0	0.0005	0	0.0009	0	0.0008	0	0.0009	0
9	0	0	0.0006	0	0.0008	0	0.0007	0	0.0007	0

Table 2: Table of the power coupling coefficients for a cornercube mixer in standard configuration (see Tab. 1)
Relative mode power $P_{sum}/P_{CC} = 63$ %

m n	0	1	2	3	4	5	6	7	8	9
0	0.7720	0	0.0107	0	0.0034	0	0.0005	0	0.0001	0
1	0.0005	0	0.0011	0	0.0006	0	0.0003	0	0.0001	0
2	0.0100	0	0.0007	0	0.0001	0	0.0001	0	0.0001	0
3	0.0090	0	0.0012	0	0.0003	0	0.0001	0	0	0
4	0.0079	0	0.0015	0	0.0003	0	0.0003	0	0.0001	0
5	0.0103	0	0.0013	0	0.0002	0	0.0001	0	0	0
6	0.0047	0	0.0012	0	0.0005	0	0.0002	0	0.0001	0
7	0.0053	0	0.0009	0	0.0003	0	0	0	0	0
8	0.0045	0	0.0008	0	0.0004	0	0.0001	0	0.0001	0
9	0.0031	0	0.0006	0	0.0002	0	0	0	0	0

Table 3: Table of the power coupling coefficients for a cornercube mixer in commercial configuration (see Tab. 1)
Relative mode power $P_{sum}/P_{CC} = 86\ \%$

m n	0	1	2	3	4	5	6	7	8	9
0	0.8797	0	0.0002	0	0.0095	0	0.0047	0	0.0010	0
1	0	0	0.0007	0	0.0002	0	0	0	0	0
2	0.0011	0	0.0074	0	0.0034	0	0.0008	0	0.0002	0
3	0	0	0	0	0	0	0	0	0	0
4	0.0179	0	0.0032	0	0.0006	0	0.0002	0	0.0001	0
5	0.0001	0	0	0	0	0	0	0	0	0
6	0.0076	0	0.0007	0	0.0002	0	0.0001	0	0.0001	0
7	0.0001	0	0	0	0	0	0	0	0	0
8	0.0019	0	0.0003	0	0.0002	0	0.0001	0	0.0001	0
9	0	0	0	0	0	0	0	0	0	0

Table 4: Table of the power coupling coefficients for a cornercube mixer in optimum configuration (see Tab. 1)
Relative mode power $P_{sum}/P_{CC} = 95\ \%$

4 Conclusions

The performance of the standard cornercube Schottky-diode mixer could be highly improved by relatively simple changes in the antenna and beam parameters. In an optimum configuration its optical coupling efficiency reaches the performance of horn antennas. Especially for frequencies higher than 600 GHz it is expected that the cornercube configuration performs better than waveguide Schottky-diode mixers because no waveguide losses occur.

Acknowledgement

This work was proposed by Prof. Dr.-Ing. H.Brand and has been supported by the Deutsche Forschungsgemeinschaft (DFG) under project number Br 522/14.

References

[1] Titz, R.U., Auel, B.; Esch, W.; Röser, H.P.; Schwaab, G.W.: *Antenna Measurements of Open Structure Schottky Mixers and Determination of Optical Elements for a Heterodyne System*, Infrared Physics, November 1989

[2] Kelly, W.M.; Vizard, D.R.; Donné, A.J.H.; Kim, S.K.: *Thermonuclear Plasma Diagnostics using Corner Cube Mixer Arrays*, Mikrowellen & HF Magazin, Vol. 15, No. 3, 1989

[3] Hartmann, G.K.; Künzi, K.F.; Schwartz, P.R.: *Millimeterwellen-Atmosphären-Sondierer (MAS) für den Einsatz auf Space Shuttle*, Mikrowellen Magazin, Vol. 11, No. 3, 1985

[4] Titz, R.U., Röser, H.P.; Schwaab, G.W.; Neilson, H.J.; Wood, P.A.; Crowe, T.W.; Peatman, W.C.B.; Prince, J.; Deaver, B.S.; Alius, H.; Dodel, G.: *Investigation of GaAs Schottky Barrier Diodes in the THz Range*, International Journal of Infrared and Millimeter Waves, Vol. 11, No. 6, 1990

[5] Keen, N.; Ediss, G.: *Measurements of a Waveguide Schottky-Barrier Mixer at 690 GHz*, Proceedings of the 21st European Microwave Conference, Stuttgart, Germany, 1991, pp. 243-246

[6] Matarrese, L.M.; Evenson, K.M.: *Improved Coupling to Infrared Whisker Diodes by Use of Antenna Theory*, Applied Physics Letters, Vol. 17, No. 1, July 1970

[7] Kräutle, H.; Sauter, E.; Schultz, G.V.: *Antenna Characteristics of Whisker Diodes used as Submillimeter Receivers*, Infrared Physics, Vol. 17, 1977, pp. 477-483

[8] Kräutle, H.; Sauter, E.; Schultz, G.V.: *Properties of a Submillimeter Mixer in an Open Structure Configuration*, Infrared Physics, Vol. 18, 1978, pp. 705-712

[9] Herrmann, Karl: *Untersuchungen zum Submillimeterwellen-Empfang bei 600 GHz mit dem System Wisker-Antenne/Schottky-Diode*, Dissertation, Universität Erlangen-Nürnberg, Erlangen, 1984

[10] Kelly, W.M.; Gans, M.J.; Eivers, J.G.: *Modelling the Response of Quasi-Optical Corner Cube Mixers*, SPIE Vol. 598, Instrumentation for Submillimeter Spectroscopy (1985),pp. 72-77

[11] Grossman, E.N.: *The coupling of Submillimeter Corner-Cube Antennas to Gaussian Beams*, Infrared Physics, Vol. 29, No. 5, pp. 875-885, 1989

[12] Brune, J.: *An Open Structure 600 GHz Mixer with Broadband IF Output Coupling*, Proceedings of the 21st European Microwave Conference, Stuttgart, Germany, 1991, pp. 247-252

[13] Simonyi, K.: *Theoretische Elektrotechnik*, VEB Deutscher Verlag der Wissenschaften, Berlin 1989

[14] Schwarz, S.E.: *Efficiency of Quasi-Optical Couplers*, International Journal of Infrared and Millimeter Waves, Vol. 5, No. 12, 1984

[15] Voges, E.: *Hochfrequenztechnik*, Band 2, Hüthig Verlag, Heidelberg, 1987

[16] Marcuse, D.: *Light Transmission Optics*, Van Nostrand Reinhold, New York 1972

[17] Kimel, I.; Elias, L.R.: *Relations between Hermite and Laguerre Gaussian Modes*, IEEE Journal of Quantum Electronics, Vol. 29, No. 9, September 1993

[18] N.N.: *Farran Technology Product Catalogue*, Edition 1990

[19] Brune, J.: *A Flexible Quasi-Optical System for Polarimetric Submillimeter-Wave Reflectometry*, IEEE Transactions on Microwave Theory and Tehniques, Vol. 40, No. 12, December 1992, pp. 2321-2324